

Characteristics of radiation fluxes of casuarina coastal shelterbelt in Zhanjiang, Guangdong province

Wei Long · Zhang Fangqiu · Gao Changjun · Cai Jian · Yi Xiaoqing

Abstract Casuarina shelterbelt is a typical forest ecosystem in tropical and south subtropical coastal zone and island of China. Solar radiation is an important factor for forest carbon sequestration and microclimate formation. Based on the radiation data of a typical *Casuarina equisetifolia* shelter forest in Zhanjiang, Guangdong province, from January to December 2010, the radiation flux characteristics were analyzed. The results showed that: (1) Gross short-wave radiation ($K\downarrow$) and Net radiation (R_n) in 2010 were 5 537.42 and 6 027.17 MJ·m⁻², of which 62.72% and 61.73% in monsoon respectively. (2) The short-wave reflectivity of the ecosystem changes mainly within the range of 8% to 15% throughout the year. (3) Effective long-wave radiation (L_n) was negative throughout the year. It showed that the air temperature is higher than canopy surface temperature all the year round. This is helpful to the water vapor condensation on the plant surface. And it is a major water source of

the coastal and island ecosystem.

Keywords Coastal island · Casuarina · Shelterbelt · Radiation flux · Short-wave reflectivity

Introduction

Coastal shelterbelt establishes the forefront of coastal zones and islands. It can change the physical characteristics of the underlying surface of the sea and land boundary, and affect the energy flow and material circulation of the sea-land ecosystem (Bonan, 2008; Finnigan, 2000). *Casuarina equisetifolia* is mainly distributed in Australia, Southeast Asia, and the Pacific Islands. More than 100 years ago, *C. equisetifolia* was introduced to China and it has become the most typical shelter tree species in the South China coastal and island sandy coast (Zhong et al. 2005; Xu et al. 2012).

Solar radiation is the most important source of energy for the earth. It can be absorbed by plant through photosynthesis and converted into chemical energy. The radiation can drive evapotranspiration, heat exchange of environment. Solar radiation is absorbed in the atmosphere or the ground through heat conduction and is the basis of meteorological change and the formation of the earth's climate (He, 2006; Anderson, 1970).

There is little research on long-term systematic obser-

Project funding Guangdong forestry science and technology innovation projects (2013KJCX011-01, 2015KJCX024) and State Forestry Bureau platform operation subsidy project (2016-LYPT-DW-074).

✉ Wei Long
weilong@sinogaf.cn

Guangdong Provincial Key Laboratory of Silviculture, Protection and Utilization / Guangdong Academy of Forestry, Guangzhou, Guangdong 510520, China

vations on the radiation balance of the *C. equisetifolia* protection forest ecosystem (Sudmeyer & Scott, 2002). In this study, the radiological data of long-term continuous observation of *C. equisetifolia* forest in coastal islands were obtained, and the radiation characteristics of *C. equisetifolia* forest ecosystem for typical coastal islands were analyzed in Guangdong province.

Materials and methods

Study area

The experimental area (110°31'30"E, 20°58'50"N) is in observation site in the coastal protection forest ecosystem of National Forestry Administration, Zhanjiang city, Guangdong province, with an average elevation of 8 m. The area has a typical monsoon climate with annual rainfall of 1 700 mm, of which more than 75% falling from April to September. The annual average temperature is 23.5 °C and average relative humidity is 80%. According to statistics, in the past 50 years, 63% of tropical cyclones in Guangdong have landed in western Guangdong, especially Zhanjiang city (He et al. 2003). The average height of the forest was 16 m, the average diameter at breast height was 17 cm, the average crown diameter was 2.8 m, and the canopy density was 0.8. The forest soil was sand resulted from coastal tidal accumulation.

Observation methods

The triangular prism micro-meteorological observation tower with a height of 25 m and a width of 50 cm was set up in the casuarina coastal shelterbelts (average height of canopy of *C. equisetifolia* was 16 m). The radiation observer NR01 (KIPP & ZONEN, Holland) is mounted on an extension arm with 1.5 m in length at 25 m above the top of the tower, and the data acquisition and storage are carried by Campbell's CR1000 Data Collector (CSI, USA). In 2010, the data was recorded every half hour. According to the monsoon climate characteristics of Guangdong province in southern China, the data of the rainy season (from April to September)

and the dry season (from January to March & from October to December) were compared. The missing data due to sensor failure was filled based on lengths of the data gaps. Single data missing was filled with linear interpolation through the previous and following data points while the longer gaps were filled with means of data obtained from same time on previous and following days. The interpolated data only accounts for 0.001% of the total data. The total amount of radiation in one year is the sum of the annual radiation, and the diurnal variation of the radiation flux takes the average of the recorded data for each year.

Theoretical framework of radiation balance

According to the theory of radiation transmission, the net radiation of the boundary layer of forest ecosystem is expressed as:

$$R_n = (K \downarrow + L \downarrow) - (K \uparrow + L \uparrow)$$

Where R_n is the net radiation, $K \downarrow$ is the total solar radiation, $L \downarrow$ is the atmospheric reverse radiation, $K \uparrow$ is the short-wave radiation reflected by the underlying surface, $L \uparrow$ is the long-wave radiation of the underlying surface, $K \downarrow + L \downarrow$ is downward radiation and $K \uparrow + L \uparrow$ is upward radiation relative to the observation interface, respectively.

Net radiation can also be expressed as:

$$R_n = (1 - r) K \downarrow - L_n$$

Where r is the short-wave reflectivity of underlying surface; L_n is the effective long-wave radiation of underlying surface. The reflectivity and the underlying surface of the long-wave effective radiation can be expressed as:

$$r = K \uparrow / K \downarrow$$

$$L_n = L \uparrow - L \downarrow$$

Data analysis

Using Microsoft excel 2010 for data analysis.

Results

Radiation flux and distribution characteristics of *C. equisetifolia* coastal shelter forest

Except for L_n , the rest radiation components are positive and the values in rainy season are higher than that in the dry season (Table 1). The total shortwave radiation in 2010 was $5\,537.42\text{ W}\cdot\text{m}^{-2}$, and the total net radiation was $6\,027.17\text{ W}\cdot\text{m}^{-2}$. The proportion of total rainy season solar radiation and net radiation accounted for 62.72% and 61.73% of total annual amount, respectively.

Diurnal variation of shortwave radiation fluxes of *C. equisetifolia* forest in dry season and rainy season

The solar shortwave radiation and reflected radiation flux showed a single peak curve or diurnal change over a day, but the shortwave solar radiation changed day by day compared with reflected radiation (Fig. 1). The average flux of shortwave solar radiation began to rise rapidly starting at 6:30 and peak at $719.61\text{ W}\cdot\text{m}^{-2}$ around 13:00 in the rainy season, then declined to 0 at 19:30. The rapid rising time in the dry season was 1 h later than in the rainy season and reached the highest value of $501.341\text{ W}\cdot\text{m}^{-2}$ at 13:30, reached daily peak an hour later but dropped sharply to zero at 19:00 half an hour earlier than that in the rainy season. The reflection radiation is basically synchronized with that of solar shortwave radiation with flat shape. The peak is $57.57\text{ W}\cdot\text{m}^{-2}$ at 12:30 and $46.28\text{ W}\cdot\text{m}^{-2}$ at 13:30 during the rainy season.

Diurnal variation of longwave radiation fluxes in dryland and rainy season over coastal shelter Forest

The diurnal variation in long-wave radiation fluxes in the atmosphere and the underlying surface showed a

gentle asymmetric single-peak change pattern, which rising rapidly in the morning and then decreasing slowly until midday to reach the valley. Atmospheric downward radiation flux is higher than that of the underlying surface upward longwave radiation flux (Fig. 2). Atmospheric reverse radiation and long-wave surface fluxes in the rainy season are higher than those in the dry season. The peak and valley values in the dry season are 1 h later than in the rainy season. Atmospheric reverse radiation flux in dry and the rainy season was the lowest at 6:00 am with $475.80\text{ W}\cdot\text{m}^{-2}$ and $425.36\text{ W}\cdot\text{m}^{-2}$, respectively, and reached a daily high $523.95\text{ W}\cdot\text{m}^{-2}$ at 13:00 and $460.14\text{ W}\cdot\text{m}^{-2}$ at 15:00, respectively. In contrast, atmospheric reverse radiation flux in the rainy season was the lowest at 6:00 am ($475.80\text{ W}\cdot\text{m}^{-2}$), the highest (for $523.95\text{ W}\cdot\text{m}^{-2}$) at 13:00 pm compared to the lowest at 6:00 am ($425.36\text{ W}\cdot\text{m}^{-2}$), the highest $460.14\text{ W}\cdot\text{m}^{-2}$ at 15:00 in the dry season. The long-wave radiation flux on the underlying surface is the lowest at 6:00 am, $475.80\text{ W}\cdot\text{m}^{-2}$ and the highest $523.95\text{ W}\cdot\text{m}^{-2}$ at 13:00 pm in the rainy season, the lowest $425.36\text{ W}\cdot\text{m}^{-2}$ at 6:00 am, and the highest $460.14\text{ W}\cdot\text{m}^{-2}$ at 15:00 pm in the dry season.

Longwave effective radiant flux was negative in the rainy and dry seasons of the year, being the highest at 5:30 in the morning, which was $-24.27\text{ W}\cdot\text{m}^{-2}$ and $-21.43\text{ W}\cdot\text{m}^{-2}$ respectively. The longwave effective radiation flux reached the lowest at $-44.96\text{ W}\cdot\text{m}^{-2}$ at 16:00 in the rainy season and $-37.24\text{ W}\cdot\text{m}^{-2}$ at 16:30 in the dry season. There were four distinct changing processes in the rainy season, rapidly decreasing from 5:30 to 11:00 am, fluctuating between 11:00 and 17:00, and rising rapidly from 17:00 to 19:30, and rising slowly between 17:30-5:30. And the dry season pattern was different with two obvious patterns, declining from 7:00-16:30 and slowly rising from 16:30 to 7:00.

Table 1 Radiation flux measured above a *C. equisetifolia* protection forest ($\text{W}\cdot\text{m}^{-2}$)

Item	$K\downarrow$	$K\uparrow$	$L\downarrow$	$L\uparrow$	L_n	R_n
rainy season	3473.10	302.59	7868.41	7318.32	-550.09	3720.62
dry season	2064.32	201.92	6917.47	6473.32	-444.15	2306.55
total	5537.42	504.50	14785.88	13791.64	-994.24	6027.17
The proportion of the rainy season (%)	62.72	59.98	53.22	53.06	55.33	61.73

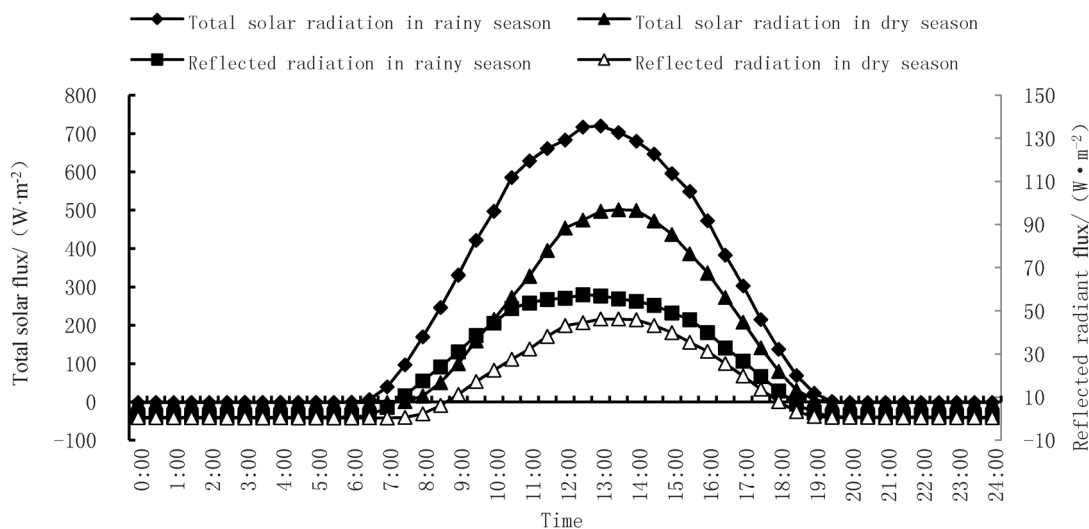


Fig.1 Diurnal variation of shortwave radiation flux in dry season and rainy season of *C. equisetifolia* forest

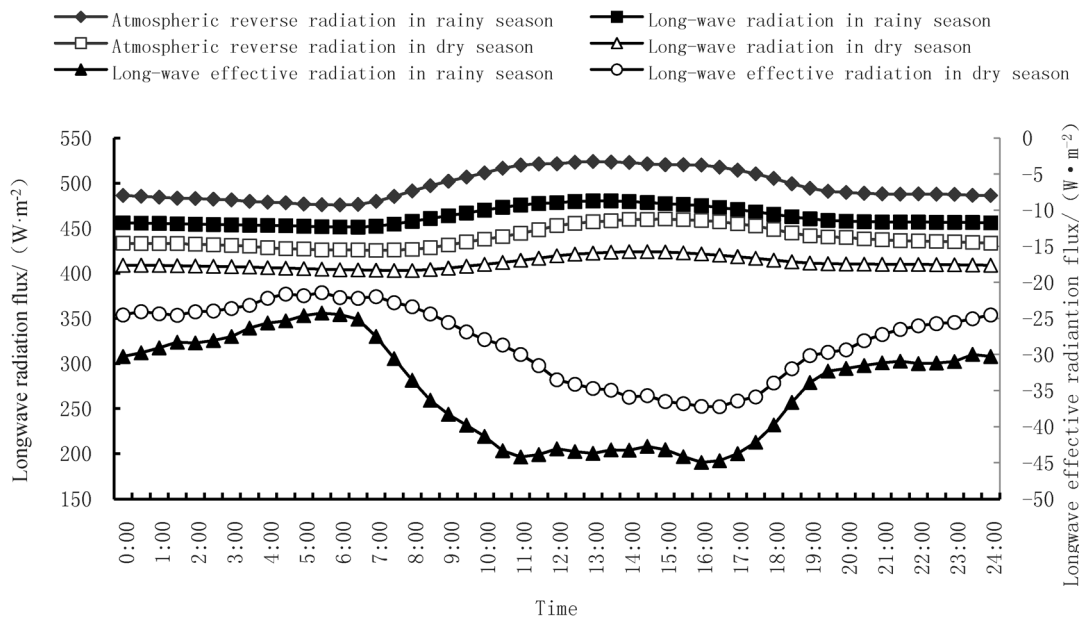


Fig.2 Diurnal variation of longwave radiation flux in dry season and rainy season of *C. equisetifolia* forest

Diurnal variation in net radiation flux in dry season and rainy season of coastal shelter forest

The diurnal variation in net radiation flux showed a single peak curve, being higher in the rainy season than that in dry season (Fig. 3). The average net radiation flux began to rise rapidly after 6:30 in the rainy season, rising to 706.30 W·m⁻² the highest at 13:00, approaching the absolute value of the effective wave of the long wave after 19:00 and the near-zero condition at night.

The rapid rise time was 1 h later in dry season than in the rainy season. The highest flux value 490.32 W·m⁻² occurred at 13:30 in the rainy season, and the peak time lagged half an hour than in the dry season.

Solar shortwave reflectivity of casuarina coastal shelter forest

In the rainy season, the half-hour reflectivity of sunrise and sunset were 0.26 and 0.72, respectively. In contrast,

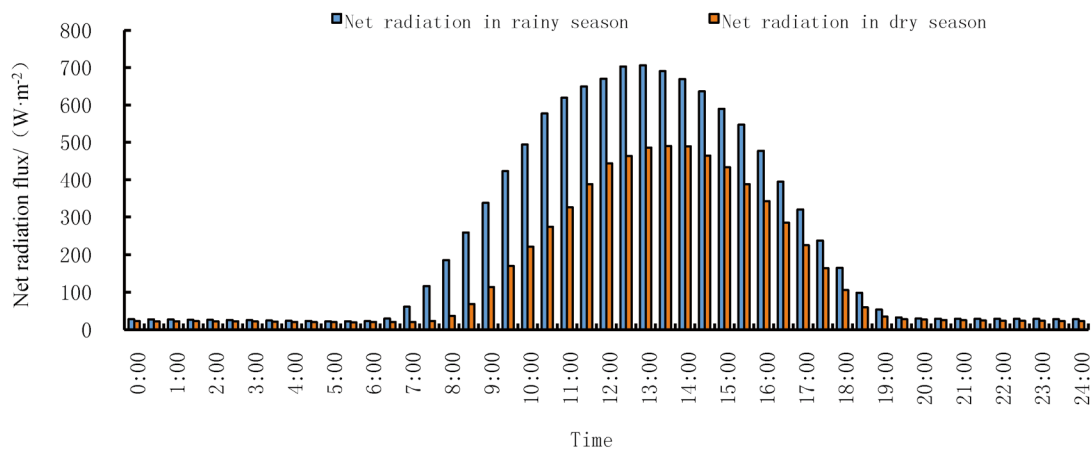


Fig.3 Diurnal variation of net radiation flux in dry season and rainy season of *C. equisetifolia* forest

the half-hour reflectivity of sunrise and sunset in the dry season were 0.60 and 0.19, respectively. The reflectivity of shortwave radiation fluctuated between 0.08 and 0.13, and the reflectivity of the shortwave radiation during the dry season was higher than that in the rainy season (Fig. 4).

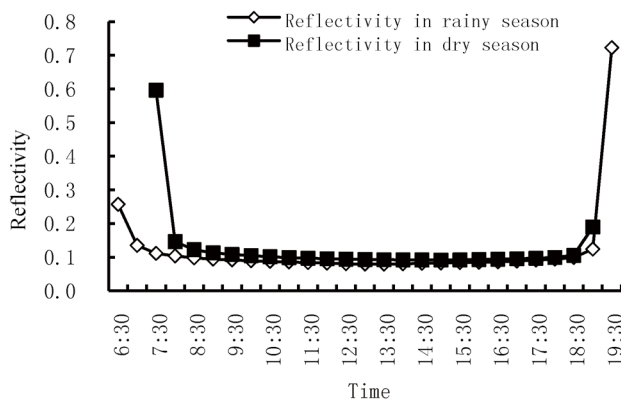


Fig.4 Diurnal variation of reflectivity in dry season and rainy season of *C. equisetifolia* forest

Discussion

Heterogeneity of radiation component variation

Solar radiation is negatively correlated with latitude and positively correlated with altitude. The total solar radiation over the Casuarina Coastal Shelterbelt (20.98°N) is $5\,537\text{ W}\cdot\text{m}^{-2}$, $519\text{ W}\cdot\text{m}^{-2}$ higher than the solar radiation over the tropical seasonal rainforest (21.95°N) in

Xishuangbanna, and is $817\text{ W}\cdot\text{m}^{-2}$ higher than that over the evergreen broad-leaved forest (23.28°N) in Mao-feng mountain of Guangzhou. According to the theory, the solar radiation decreased by $42\text{ W}\cdot\text{m}^{-2}$ every one degree increase of the latitude while the solar radiation in Donghai Island (8 m above sea level) is much higher than that of the two places. This may be related to the environmental meteorological factors such as the fog of Xishuangbanna tropic rain forest and the haze of Mao-feng mountain in the city of Guangzhou. The impacts weakened the solar radiation (Chen et al. 2011; Zhang et al. 2005; Tan et al. 2015). The above phenomenon shows the importance of actual long-term observation.

Variation in shortwave reflectivity on the underlying surface

The surface albedo plays an important role in the energy allocation of the earth-air system, which has a direct impact on the global and regional climate and the carbon fixation effect of the plantation (Betts, 2000; Zhao & Zeng 2002).

The shortwave reflectance of the casuarina protection forest is mainly determined by the position of the sun and earth in Donghai Island. The reflectivity decreases as the height of the sun increases. The reflectivity during sunrise and sunset is much higher than during the day. The height of the sun in the northern hemisphere increased and the reflectivity of the underlying surface decreased. Many studies have shown that the reflection of the underlying surface against solar radiation also

depends on the underlying properties and states, such as vegetation types, soil types and water conditions that affect surface roughness (Liang et al. 2002; Zhang et al. 2015). After the degradation of *C. equisetifolia* leaves, the photosynthetic green branches like the coniferous leaves were formed. And the underlying surface reflectivity of the tropical and south subtropical evergreen forest ecosystems with the dominant tree species of *C. equisetifolia* was higher in dry season than that of the rainy season. In the dry season, the older branch of *C. equisetifolia* falls result in the leaf area index and the roughness of the underlying surface decreased, and the dryness increased, which caused the rising of the reflectivity. The studied show that the reflectivity of dry sand is 35%–45%, sand soil is 29%–35%, coniferous forest is 5%–10% and deciduous forest is 10%–20% (Yu & Sun, 2006). *Casuarina* protection forest is a single dominant tree species community set on the original tidal formed sandland. The solar shortwave radiation reflectivity is between 8% and 15% in Donghai Island. After the establishment of artificial community, a new biogeochemical cycle system including interlayer plants, understory vegetation and soil has been formed during the succession. This changes the radiation characteristics of the surface and canopy and improves the solar energy utilization rate.

Effects of radiation flux change and its distribution on shelter forest ecosystem

The solar total radiation, atmospheric radiation, and net radiation over *C. equisetifolia* coastal shelterbelt are higher in the dry season than in the rainy season in Donghai Island. The net radiation is higher than total radiation throughout the year. Coastal and island shelterbelt is in the marine-terrestrial ecotone, and the sea-land breeze dominated near-surface layer atmospheric movement brings a lot of water vapor to the coastal zone to produce more cloud cover. These clouds and other aerosols absorb the long-wave radiation of the sun and that reflected from the underlying surface, forming a strong greenhouse effect (Chapin et al, 2011).

Long-wave effective radiation is negative throughout the year. This indicated that the underlying surface ab-

sorb energy through the atmosphere reverse radiation. The smaller the value, the more energy is absorbed by the underlying surface from the reverse radiation (Chapin et al, 2011; Ramanathan et al. 2001). It also indicates that the atmospheric temperature is higher than the underlying surface temperature of the interfacial layer of the protective forest ecosystem, which is conducive to the condensation of large amounts of water contained in the atmosphere on the surface of the vegetation when the solar radiation is zero at night (Dale et al. 2000). For the shelter forest plant forefront of the high tide line, more physiological stress caused by the salt spray condensed on the trunk and leaf would appear. From another perspective, this physical obstruction against salt spray is also an important ecological function of shelter forest (Boyce, 1954; Buijnzeel & Veneklaas, 1998).

Radiation balance is a regular eco-environmental index. Theoretically, the radiation and reflection characteristics of a place can be predicted by sun-earth relationship and geo-location. But the radiation characteristic is affected by cloud cover, surface vegetation and water conditions, and heat flux of sea-land exchange and so on. The basic data on the radiation balance of coastal and island shelterbelt are scarce. Data based on field observation are the basis of tree species ecological adaptation, coastal ecological restoration, meteorological and climate disaster research (Jackson et al. 2008; Tian et al. 2010; D'Amato et al. 2011). Long-term monitoring data of forest radiation can improve the remote sensing monitoring of forest resources and the accuracy of land surface model parameters.

Reference

- Anderson MC (1970) Interpreting the fraction of solar radiation available in forest. *Agricultural Meteorology* 7(70): 19–28
- Betts RA (2000) Offset of the potential carbon sink from boreal forestation by decreases in surface albedo. *Nature* 408(6809): 187–190
- Bonan GB (2008) Forests and climate change: Forcings, feedbacks, and the climate benefits of forests. *Science* 320(5882): 1444–1449
- Boyce SG (1954) The salt spray community. *Ecological monographs* 24(1): 29–67

- Bruijnzeel LA, Veneklaas EJ (1998) Climatic conditions and tropical montane forest productivity: the fog has not lifted yet. *Ecology* 79(1): 3-9
- Chapin IIF, Matson PA, Vitousek P (2011) Principles of terrestrial ecosystem ecology. New York: Springer Science & Business Media
- Chen J, Chen BF, Pan YJ, et al (2011) Characteristics of radiation fluxes of an evergreen broad-leaved forest in Maofeng Mountain, Guangzhou, China. *Acta Ecologica Sinica* 22: 6766-6776
- D'Amato AW, Bradford JB, Fraver S, et al (2011) Forest management for mitigation and adaptation to climate change: Insights from long-term silviculture experiments. *Forest Ecology and Management* 262(5): 803-816
- Dale VH, Brown S, Haeuber RA, et al (2000) Ecological principles and guidelines for managing the use of land. *Ecological applications* 10(3): 639-670
- Finnigan J (2000) Turbulence in plant canopies. *Annual Review of Fluid Mechanics* 32(1): 519-571
- He HY, Jian MQ, Song LL (2003) Some Climatic Features of the Tropical Cyclones Landed onto Guangdong Province During the Recent 50 Years. *Scientia Meteorologica Sinica* 23(4): 401-409
- He QT (2006) *Meteorology (Revised Edition)*. Beijing: China Forestry Publishing House
- Jackson RB, Randerson JT, Canadell JG, et al (2008) Protecting climate with forests. *Environmental Research Letters* 3(4): 044006
- Liang S, Fang H, Chen M, et al (2002) Validating MODIS land surface reflectance and albedo products: Methods and preliminary results. *Remote sensing of environment* 83(1): 149-162
- Ramanathan V, Crutzen PJ, Kiehl JT, et al (2001) Aerosols, climate, and the hydrological cycle. *science* 294(5549): 2119-2124
- Sudmeyer RA, Scott PR (2002) Characterisation of a windbreak system on the south coast of Western Australia. 1. Microclimate and wind erosion. *Australian Journal of Experimental Agriculture* 42(6): 11-3
- Tan ZH, Yu GR, Zhou GY, et al (2015) Microclimate of forests across East Asia biomes: 1. Radiation and energy balance. *Chinese Journal of Plant Ecology* (6): 541-553
- Tian B, Zhang LQ, Wang XR, et al (2010) Forecasting the effects of sea-level rise at Chongming Dongtan Nature Reserve in the Yangtze Delta, Shanghai, China. *Ecological Engineering* 36(10): 1383-1388
- Xu XY, Wang MH, Wei L, et al (2012) Analysis of Genetic Diversity and Relationship Among 51 Casuarina Superior Clones by Using ISSR Markers. *Forest Research* 25(6): 691-696
- Yu GR, Sun XM (2006) *Principle and Flux Measurement in Terrestrial Ecosystem*. Beijing: Higher Education Press
- Zhang C, Fan GZ, Ma ZG, et al (2015) Characteristics of Albedo over Different Underlying Surface in the Semi-Arid Area. *Plateau Meteorology* 34(4): 1029-1040
- Zhang YP, Dou JX, Yu GR, et al (2005) Characteristics of solar radiation and its distribution above the canopy of tropical seasonal rain forest in Xishuangbanna, Southwest China. *Journal of Beijing Forestry University* 27(5): 17-25
- Zhao M, Zeng XM (2002) A Theoretical Analysis on the Local Climate Change Induced by the Change of Land use. *Advances in Atmospheric Sciences* 19(1): 45-63
- Zhong CL, Bai JY, Zhang Y (2005) Introduction and Conservation of Casuarina Trees in China. *Forest Research* 18(3): 345-350